Talanta 176 (2018) 509–517

Contents lists available at ScienceDirect

Talanta

journal homepage: www.elsevier.com/locate/talanta

Intellectual modifying a bare glassy carbon electrode to fabricate a novel and ultrasensitive electrochemical biosensor: Application to determination of acrylamide in food samples

Kambiz Varmira[a], Omid Abdi[a], Mohammad-Bagher Gholivand[b], Hector C. Goicoechea[c], Ali R. Jalalvand[a,*]

[a] Research Center of Oils and Fats (RCOF), Kermanshah University of Medical Sciences, Kermanshah, Iran
[b] Department of Analytical Chemistry, Faculty of Chemistry, Razi University, Kermanshah, Iran
[c] Laboratorio de Desarrollo Analítico y Quimiometría (LADAQ), C_atedra de Química Analítica I, Universidad Nacional del Litoral, Ciudad Universitaria, CC ,242 (S3000ZAA), Santa Fe, Argentina

ARTICLE INFO

Keywords:
Acrylamide
Hemoglobin
Adduct
Biosensor
Square wave voltammetry
Food samples

ABSTRACT

Acrylamide (AA) is a neurotoxin and carcinogen which is mainly formed in foods containing large quantities of starch processed at high temperatures and its determination is very important to control the quality of foods. In this work, a novel electrochemical biosensor based on hemoglobin-dimethyldioctadecylammonium bromide (HG-DDAB)/platinum-gold-palladium three metallic alloy nanoparticles (PtAuPd NPs)/chitosan-1-ethyl-3-methylimidazolium bis(trifluoromethylsulfonyl)imide (Ch-IL)/multiwalled carbon nanotubes-IL (MWCNTs-IL)/glassy carbon electrode (GCE) is proposed for ultrasensitive determination of AA in food samples. Development of the biosensor is based on forming an adduct by the reaction of AA with α-NH_2 group of N-terminal valine of HG which decreases the peak current of HG-Fe^{+3} reduction. The modifications were characterized by electrochemical impedance spectroscopy (EIS), cyclic voltammetry (CV), energy dispersive X-ray spectroscopic (EDS) and scanning electron microscopy (SEM). Under optimized conditions, the biosensor detected AA by square wave voltammetry (SWV) in two linear concentration ranges of 0.03–39.0 nM and 39.0–150.0 nM with a limit of detection (LOD) of 0.01 nM. The biosensor was able to selective detection of AA even in the presence of high concentrations of common interferents which confirmed that the biosensor is highly selective. Also, the results obtained from further studies confirmed that the proposed biosensor has a short response time (less than 8 s), good sensitivity, long term stability, repeatability, and reproducibility. Finally, the proposed biosensor was successfully applied to determine AA in potato chips and its results were comparable to those obtained by gas chromatography-mass spectrometry (GC-MS) as reference method.

1. Introduction

Acrylamide (AA, Fig. 1A) is a vinylic compound with a low molecular weight which is both colorless and odorless, and is highly soluble in water, easily reactive in air, and rapidly polymerizable [1]. The AA derives from a reaction between proteins/aminoacids (mainly asparagine) and reducing sugars which is called Maillard reaction [2]. In 2002, Swedish National Food Administration and Stockholm

Abbreviations: AA, acrylamide; FAO/WHO, food and agriculture organization of the united nations and world health; HS-SPME-GC-FID, headspace solid-phase microextraction-gas chromatography-flame ionization detection; LC-MS/MS, liquid chromatography-tandem mass spectrometry; SPE-HPLC-MS/MS, solid phase extraction-high performance liquid chromatography tandem mass spectrometry; HPLCMS/MS, high performance liquid chromatography-tandem mass spectrometry; GC-ECD, gas chromatography-electron capture detector; SPME-GC-PCI-MS-MS, solid phase microextraction-gas chromatography-positive chemical ionization tandem mass spectrometry; GC-IT/MS, gas chromatography-ion trap mass spectrometry detector; DLLME, dispersive liquid-liquid microextraction; GC-ECD, followed by gas chromatography-electron capture detector; RP-DISDME-GC, reversed phase-direct immersion single drop microextraction-gas chromatography; RP-HPLC-DAD, reversed phase-high performance liquid chromatography-diode array detector; HG, hemoglobin; GCE, glassy carbon electrode; CNTs, carbon nanotubes; ILs, ionic liquids; RTILs, room temperature ionic liquids; NPS, nanoparticles; Pt, platinum; Au, gold; Pd, palladium; Ch, chitosan; DDAB, dimethyldioctadecyl-ammonium bromide; DDW, doubly distilled deionized water; DMF, dimethylformamide; EIS, electrochemical impedance spectroscopy; SWV, square wave voltammetry; EDS, energy dispersive X-ray spectroscopy; AsLSSR, asymmetric least square spline regression; EJCR, elliptical joint confidence region; CV, cyclic voltammetry; OLS, ordinary least squares; RSD, relative standard deviation; I, peak intensity; C_{AA}, concentration values of AA samples; LOD, limit of detection; SEM, scanning electron microscope; R_{ct}, electron transfer resistance; PDB, protein data bank

* Corresponding author.
E-mail address: ali.jalalvand1984@gmail.com (A.R. Jalalvand).

http://dx.doi.org/10.1016/j.talanta.2017.08.069
Received 3 August 2017; Received in revised form 19 August 2017; Accepted 21 August 2017
Available online 24 August 2017
0039-9140/

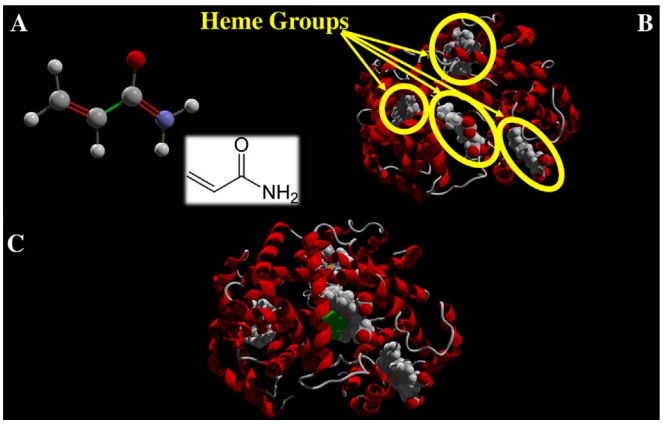

Fig. 1. (A) Molecular structure of AA, (B) secondary structure of HG and (C) the computer-generated model of AA (shown as CPK in green) bound to 1142 heme group of HG (HG-AA adduct). (For interpretation of the references to color in this figure legend, the reader is referred to the web version of this article.)

University reported the existence of high concentrations of AA in various foodstuffs, particularly in potato products processed at high temperatures [3,4]. According to the scientific reports, AA is a human carcinogen which causes neural destructions in people who are exposed to it [5,6]. According to the reports of Food and Agriculture Organization of the United Nations and World Health Organization (FAO/WHO), 0.3–0.8 μg kg^{-1} body $weight^{-1}$ day^{-1} is the daily intake of AA from the foods and values higher than this can cause toxic effects on humans [7]. Therefore, determination of AA in foods is crucial for controlling the quality of foods.

Too many analytical methods such as headspace solid-phase microextraction-gas chromatography-flame ionization detection (HS-SPME-GC-FID) [8], liquid chromatography-tandem mass spectrometry (LC-MS/MS) [9], solid phase extraction-high performance liquid chromatography tandem mass spectrometry (SPE-HPLC-MS/MS) [10] and HPLC-MS/MS [11] have been developed to determine the AA in foods. GC-electron capture detector GC-ECD [12], solid phase microextraction-GC-positive chemical ionization tandem mass spectrometry (SPME-GC-PCI-MS-MS) [13], GC-ion trap mass spectrometry detector (GC-IT/MS) [12], dispersive liquid-liquid microextraction (DLLME) followed by GC-ECD [14], reversed phase-direct immersion single drop microextraction-GC (RP-DISDME-GC) [15], reversed phase- HPLC-diode array detector (RP-HPLC-DAD) [16], and LC coupled with electrochemical detection [17] have also been developed to determine the AA in foods. All of the mentioned techniques are too expensive and time-consuming and in some of them derivatization of AA by bromination is needed which could be a source of artifacts. In addition to the mentioned problems, most of these techniques has a complex step for sample preparation which causes discrepancies between determinations. The mentioned disadvantages and, at the same time, growing demand for low-cost and sensitive determination of AA in food samples, has motivated the analytical chemists to develop novel and suitable techniques for screening this neurotoxic compound. Among the existing analytical techniques, electrochemical biosensors because of several advantages such as simplicity, sensitivity, selectivity, rapid response, simple construction, simple operation, reliability, capability of real sample analysis, low-cost, repeatability and reproducibility can be considered as an excellent choice for determination of AA.

Hemoglobin (HG) is a redox active protein which involves four polypeptide chains and each polypeptide chain has one electroactive-Fe^{3+} heme group (Fig. 1B) [18]. The electroactivity of HG is related to the reversible conversion of HG-Fe^{3+} to Hb-Fe^{2+} . The functional groups of HG cannot be easily oxidized or reduced at bare electrodes because of the very slow electron transfer process caused by the large three-dimensional structure of the HG. Such a large structure causes unsuitable orientation of HG onto the electrode surface and increases the distance between heme centers and surface of the electrode [19,20]. Slow electron transfer can also be caused by the protein adsorption and passivation of the electrode which has been tackled by modification of the electrode using a variety of electromediators such as polymer films [21,22], poly-3-hydroxybutyrate membrane [23], carbon nanotubes [24,25], gold nanoparticles [26–32], zirconium dioxide nanoparticles [33] and agarose hydrogel films [34]. Development of the proposed biosensor in this study relays on the reaction of HG with AA which causes formation of a HG-AA adduct and can alter the electroactivity of HG. Therefore, by addition of AA to the medium, the adduct HG-AA is formed at the electrode surface which decreases the peak current of HG. Decrease of current can be regarded as the analytical signal which could be a great base for very selective determination of AA.

To increase the sensitivity of the proposed biosensor towards AA determination, suitable modification of the glassy carbon electrode (GCE) as the platform of the biosensor must be performed. Carbon nanotubes (CNTs) because of their unique electrochemical and mechanical properties such as high surface area, high electron transfer rate, high stability and minimization of the surface fouling have received a lot of attention for constructing electrochemical biosensors [35]. Another class of materials for electrochemical applications is ionic liquids (ILs) which have excellent properties such as stability, high electrical conductivity and low vapor pressure [36]. Because of π-π or cation-π interaction between CNTs and IL, the CNTs-IL composite has had potential applications in construction of electrochemical biosensor [37]. Composite films composed of room temperature ionic liquids (RTILs) and CNTs are unique materials with interesting properties for fabrication of electrochemical biosensors [38,39]. Chitosan (Ch) as a natural biopolymer has high mechanical strength and excellent ability for film forming which is biocompatible, water permeable and nontoxic [39]. Ch is able to accumulate metallic NPs by different mechanisms such as electrostatic attraction, chelation and ion exchange. For improving properties of Ch its combination with other materials such as ethylene diamine [40], thiourea [41], CNTs [42] and functionalized ILs [43] have been reported. The ILs due to having low interfacial tension are able to enhance the nucleation rate which facilitates formation of smaller NPs. Electrodeposition is a very controllable and robust method for synthesis of metal nanoparticles (NPs) by which the size, composition, density, and even the shape of NPs can be controlled via potential, concentration, time, and composition of metal precursor solutions [44]. Due to the interaction between components in alloy NPs they show interesting properties including catalytic selectivity, high catalytic activity and better resistance to deactivation in comparison with their corresponding monometallic components. Among different alloy NPs, three metallic alloys are very attractive therefore, we are going to use platinum-gold-palladium (PtAuPd) alloy NPs which can help to the adsorption of HG onto the biosensor surface due to the interaction between cysteine or $NH^{+}{}_{4}$-lysine residues of HG and Au NPs [45–47]. It has been suggested by the other researchers that the dimethyldioctadecylammonium bromide (DDAB) is able to form an ordered bilayer structure which is suitable for protein immobilization and facilitates the electron transfer between protein and electrode [48–52]. Therefore, in order to facilitate the electron transfer and enhance the concentration of HG at the electrode surface, HG in combination with DDAB was dropped onto the biosensor surface.

In this work, we are going to construct an ultrasensitive electrochemical biosensor for determination of AA in food samples based on the reaction of HG with AA to form a HG-AA adduct which is able to alter the electroactivity of HG. The platform of the biosensor is a GCE which is modified with MWCNTs-IL to increase the sensitivity of the developed biosensor. Ch-IL is the next layer onto MWCNTs-IL which accumulates metallic NPs. Then, a three-metallic alloy including Au, Pt and Pd is electrodeposited onto Ch-IL and the last layer includes HG-DDAB. Finally, the developed biosensor (HG-DDAB/PtAuPd NPs/Ch-

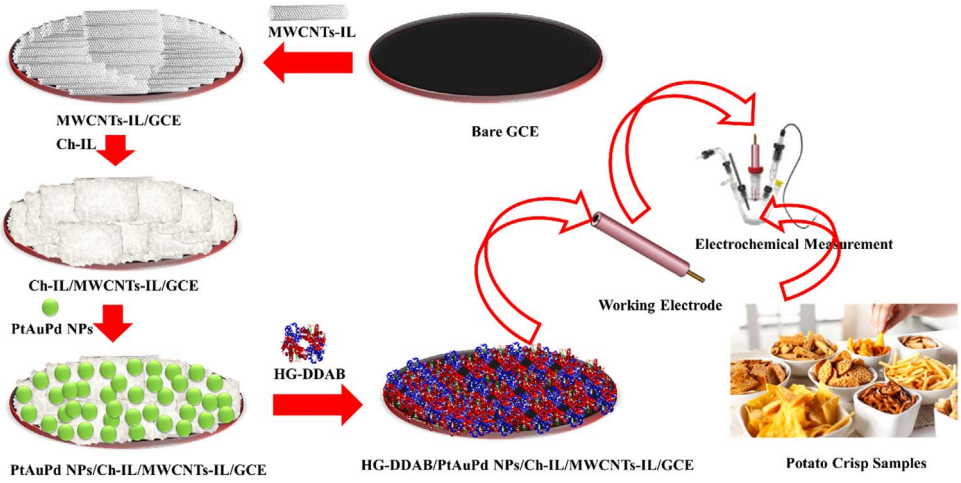

Scheme 1. Schematic representation of the fabrication steps of the proposed biosensor in this study.

IL/MWCNTs-IL/GCE) will be applied to the determination of AA in water extract from potato crisps. Schematic representation of the fabrication steps of the proposed biosensor in this study is shown in Scheme 1.

2. Experimental

2.1. Chemicals and solutions

AA, HG, DDAB, Ch, 1-ethyl-3-methylimidazolium bis(trifluoromethylsulfonyl)imide, potassium ferrocyanide, potassium ferricyanide, gold (III) tetrachloride ($HAuCl_4$), zinc sulphate heptahydrate, palladium (II) chloride ($PdCl_2$), hexachloroplatinic acid (H_2PtCl_6), zinc sulphate heptahydrate, dimethylformamide (DMF), acetic acid, sodium phosphate monobasic (NaH_2PO_4), sodium phosphate dibasic (Na_2HPO_4), phosphoric acid and sodium hydroxide were purchased from Sigma. Multi-walled carbon nanotubes (MWCNTs) were purchased from Ionic Liquid Technologies. The other reagents were purchased from regular sources and used as received. Doubly distilled deionized water (DDW) was used to prepare all the solutions. Highly pure N_2 was applied for deaeration.

A phosphate buffered solution (PBS, 0.05 M) was prepared from NaH_2PO_4, and Na_2HPO_4 and phosphoric acid and sodium hydroxide were used to adjust its pH at 7.0. The redox probe solution, $[Fe(CN)_6]^{3-/4-}$, with a concentration of 5.0×10^{-3} M was prepared in the PBS (0.05 M, pH 7.0) and used for electrochemical impedance spectroscopic (EIS) experiments. A stock solution of AA was prepared in the PBS (0.05 M, pH 7.0) with a concentration of 0.1 M, and was stored at 2 °C in a refrigerator. Working solutions of AA were prepared from its stock solution by appropriate dilutions. A stock solution of Ch (0.1%) was prepared in acetic acid (1.0% (v/v)) by ultrasonication for 40.0 min. The Ch-IL was prepared by addition of 2.0 µL IL into 2.0 mL Ch (0.1%). To prepare MWCNTs-IL, 2.0 mg MWCNTs and 2.0 µL IL were added to 2.0 mL DMF and ultrasonicated for 40.0 min. DDAB (0.01 M) was prepared in the DDW and ultrasonicated for 40.0 min to obtain a homogeneous dispersion of liposomes. HG-DDAB liposomes were prepared by mixing 250 µL DDAB liposomes (0.01 M) and 250 µL 0.1 mM HG in the PBS (0.05 M, pH 7.0) by ultrasonicating for 40.0 min. A solution containing 2.5 mM $HAuCl_4$, 2.5 mM $PdCl_2$, 2.5 mM H_2PtCl_6 and 0.1 M KCl was prepared in the DDW.

2.2. Instruments and softwares

All the electrochemical measurements including voltammetric and EIS experiments were performed by an Autolab PGSTAT302N-high performance controlled by the NOVA 2.1.2 software equipped with an electrochemical cell including three electrodes: Ag/AgCl as reference electrode, Pt wire as counter electrode and modified glassy carbon electrode (GCE) as working electrode. The SEM images were recorded by a KYKY-EM 3200 scanning electron microscope (SEM). Energy dispersive X-ray spectroscopy (EDS) were performed for elemental analysis by an EDS-integrated Hitachi S-4800. A GC-MS system including an Agilent gas chromatograph 6890 (Agilent Technologies, USA) coupled to a GCT high-resolution time-of-flight mass spectrometer (Micromass, UK), was used for AA determination in real samples with the aim of validating the developed methodology in this study. An Eppendorf centrifuge was used to centrifuging the solutions. A JENWAY-3345 pH-meter equipped with a combined glass electrode was applied to pH measurements. All the recorded electrochemical data was converted to matrices and processed in MATLAB (Version 7.14, MathWorks, Inc.). The computations based on asymmetric least squares splines regression (AsLSSR) and elliptical joint confidence region (EJCR) were performed in MATLAB environment. The known crystal structure of HG was obtained from the Brookhaven Protein Data Bank (PDB ID: 1GZX). The molecular structure of the AA was depicted by Hyperchem package (Version 8.0), and optimized by AM1semiempirical method with Polak-Ribiere algorithm. The Discovery Studio 2.5 was used to realize the binding mode of AA at the HG. All the computations were performed on a DELL XPS laptop (L502X).

2.3. Preparation of the biosensor

The GCE was polished by a silky pad in an alumina slurry, rinsed with water and ultrasonicated in ethanol for 10.0 min and dried. 5.0 µL of MWCNTs-IL was dropped onto the surface of the polished GCE by a micropipette and dried at room temperature. To prepare the Ch-IL/MWCNTs-IL/GCE, 4.0 µL of Ch-IL was dropped onto the surface of MWCNTs-IL/GCE and left to be dried at room temperature. Then, the Ch-IL/MWCNTs-IL/GCE was used as working electrode and immersed into an electrochemical cell containing 10.0 mL of a solution consisting of 2.5 mM $HAuCl_4$, 2.5 mM $PdCl_2$, 2.5 mM H_2PtCl_6 and 0.1 M KCl where Ag/AgCl and Pt wire were acted as reference and counter electrodes, respectively. Electrochemical deposition of PtAuPd alloy NPs onto the Ch-IL/MWCNTs-IL/GCE was performed with the help of cyclic voltammetry (CV) by scanning potential (scan rate = 0.025) from 0 to −0.5 V for 6 cycles. Finally, 5.0 µL of HG-DDAB was dropped on to the surface of PtAuPd NPs/Ch-IL/MWCNTs-IL/GCE and left to be dried at room temperature. The HG-DDAB/PtAuPd NPs/Ch-IL/MWCNTs-IL/GCE was covered and kept in a refrigerator until analysis time.

2.4. Preparation of real samples

For preparing the real samples, two solutions (solution I and solution II) were prepared according to the following procedures: solution I was prepared by dissolution of 15.0 g of potassium hexacyanoferrate (II) trihydrate in 50.0 mL DDW. Solution II was prepared by dissolution of 30.0 g zinc sulphate heptahydrate in 50.0 mL DDW.

Two potato crisp samples provided by two famous Iranian brands including Maz Maz and Chee Toz were selected as real cases for AA determination. 50.0 g of potato crisp samples were separately crushed by a mortar to obtain homogeneous powders and added to 500.0 mL DDW and left to be swelled for half an hour. Then, the samples were kept at 60.0 °C and shaken for one hour and centrifuged at 6000.0 rpm for about 15.0 min. The extraction with hexane was used to defatting the supernatant solutions. 10.0 mL of solutions I and II were added to the obtained aqueous solutions for purifying them and the supernatants were filtered. Finally, the pHs of the solutions were adjusted by the PBS (0.05 M, pH 7.0) and used for electrochemical measurements.

3. Results and discussion

3.1. Electrochemical characterizations of the modified electrodes by EIS and CV

The EIS is a well-known and effective electrochemical method for characterizing the features of the surface of modified electrodes. The Nyquist plot of impedance spectra involves semicircle and linear portions in which the semicircle portion corresponds to the electron transfer limited process and the linear portion corresponds to the diffusion process. The semicircle diameter refers to the electron transfer resistance (R_{ct}) of the electrode surface which can describe the interface properties of the electrode. The R_{ct} values of the EIS curves were calculated by electrochemical circle fit command provided by the NOVA software. The Nyquist plots of the GCE, MWCNTs-IL/GCE, Ch-IL/MWCNTs-IL/GCE, PtAuPd NPs/Ch-IL/MWCNTs-IL/GCE and HG-DDAB/PtAuPd NPs/Ch-IL/MWCNTs-IL/GCE were recorded in the redox probe solution and are shown in Fig. 2A. As can be seen, the EIS curve of the bare GCE (Fig. 2A, curve a) involves a big semicircle, and its R_{ct} is about 14.12 kΩ. The presence of MWCNTs-IL at the GCE enhances the electron transfer rate as is obvious from the EIS curve of MWCNTs-IL/GCE (Fig. 2A, curve b) which its R_{ct} has been reduced to 6.14 kΩ. By dropping the Ch-IL onto MWCNTs-IL/GCE surface, the R_{ct} of its EIS curve (Fig. 2A, curve c) was increased to 7.98 kΩ, which manifested that the Ch had a blocking effect on the electron transfer of the redox probe. After electrochemical deposition of PtAuPd NPs onto the surface of Ch-IL/MWCNTs-IL/GCE, the R_{ct} was dramatically decreased (1.94 kΩ, Fig. 2A, curve d) which revealed that PtAuPd NPs can provide a lot of new conduction pathways to facilitate electron transfer between electrode surface and electrolyte solution. After dropping HG-DDAB onto the surface of PtAuPd NPs/Ch-IL/MWCNTs-IL/GCE, the R_{ct} was increased to 3.80 kΩ (Fig. 2A, curve e) which showed that the HG can hinder the interfacial electron transfer in some extent.

The CV was used as another efficient technique for further characterization of the modified electrodes. At MWCNTs-IL/GCE, the redox probe showed a CV with obviously larger peak currents (Fig. 2B, curve b) than those obtained at GCE (Fig. 2B, curve a), manifesting larger electroactive surface area and faster electron transfer for MWCNTs-IL/GCE. Recording the CV of the Ch-IL/MWCNTs-IL/GCE immersed into the redox probe solution showed smaller peak currents (Fig. 2B, curve c) which confirmed that Ch can hinder the electron transfer in some extent. After electrodeposition of PtAuPd NPs onto Ch-IL/MWCNTs-IL/GCE, peak potential separation decreased while peak current dramatically increased (Fig. 2B, curve d) which confirmed the excellent role of PtAuPd NPs in expanding the electroactive surface area and fastening the rate of electron transfer. When HG-DDAB was immobilized onto the surface of PtAuPd NPs/Ch-IL/MWCNTs-IL/GCE (Fig. 2B, curve e), the peak current went down and peak separation increased which showed that the large HG molecules were able to block the interface in some extent and decrease the electron transfers rate.

3.2. Characterizations of the modified electrodes by SEM and EDS

In order to characterize the surface morphologies of the modification steps, the SEM images were captured from the surface of modified electrodes and are showing in Fig. 3. Fig. 3A shows the SEM image of MWCNTs-IL/GCE which confirms that the MWCNTs have been twinned around each other and attached to the surface of the GCE. From Fig. 3A it can be also concluded that the MWCNTs-IL homogeneously distributed onto the GCE surface and formed a thin layer. After dropping Ch-IL onto the MWCNTs-IL/GCE surface, the surface was covered by a thin film of Ch-IL which can also be confirmed by Fig. 3B. Fig. 3C shows that the surface has been decorated by NPs which also confirms the successfulness of electrochemical deposition in synthesis of PtAuPd NPs. When HG-DDAB was immobilized onto the PtAuPd NPs/Ch-IL/MWCNTs-IL/GCE surface, a film was formed and covered the biosensor surface as can be seen in Fig. 3D. Elemental compositions of electrochemically deposited PtAuPd NPs were analyzed by EDS and the results are showing in Fig. 3E. Signature peaks for Pt, Au and Pd were observed and the weight percentage of Pt, Au and Pd was 33.33%, 32.68% and 33.05%, respectively, which were in good agreement with the molar ratio of metal precursors.

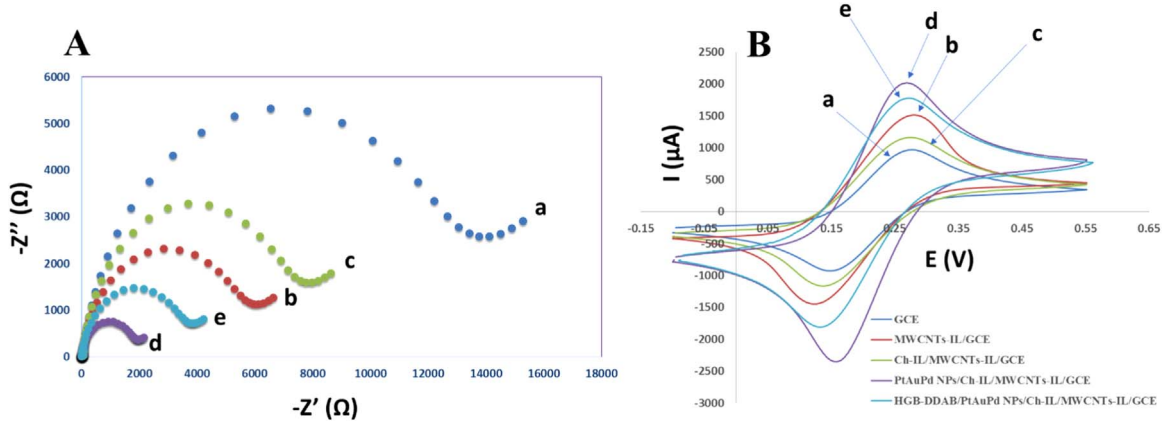

Fig. 2. (A) EISs and (B) CVs of $[Fe(CN)6]^{3-/4-}$, 5.0×10^{-3} M, in PBS (0.05 M, pH = 7.0) at a scan rate (υ) of 50.0 mVs^{-1} on (a) GCE, (b) MWCNTs-IL/GCE, (c) Ch-IL/MWCNTs-IL/GCE, (d) PtAuPd NPs/Ch-IL/MWCNTs-IL/GCE and (e) HG-DDAB/PtAuPd NPs/Ch-IL/MWCNTs-IL/GCE.

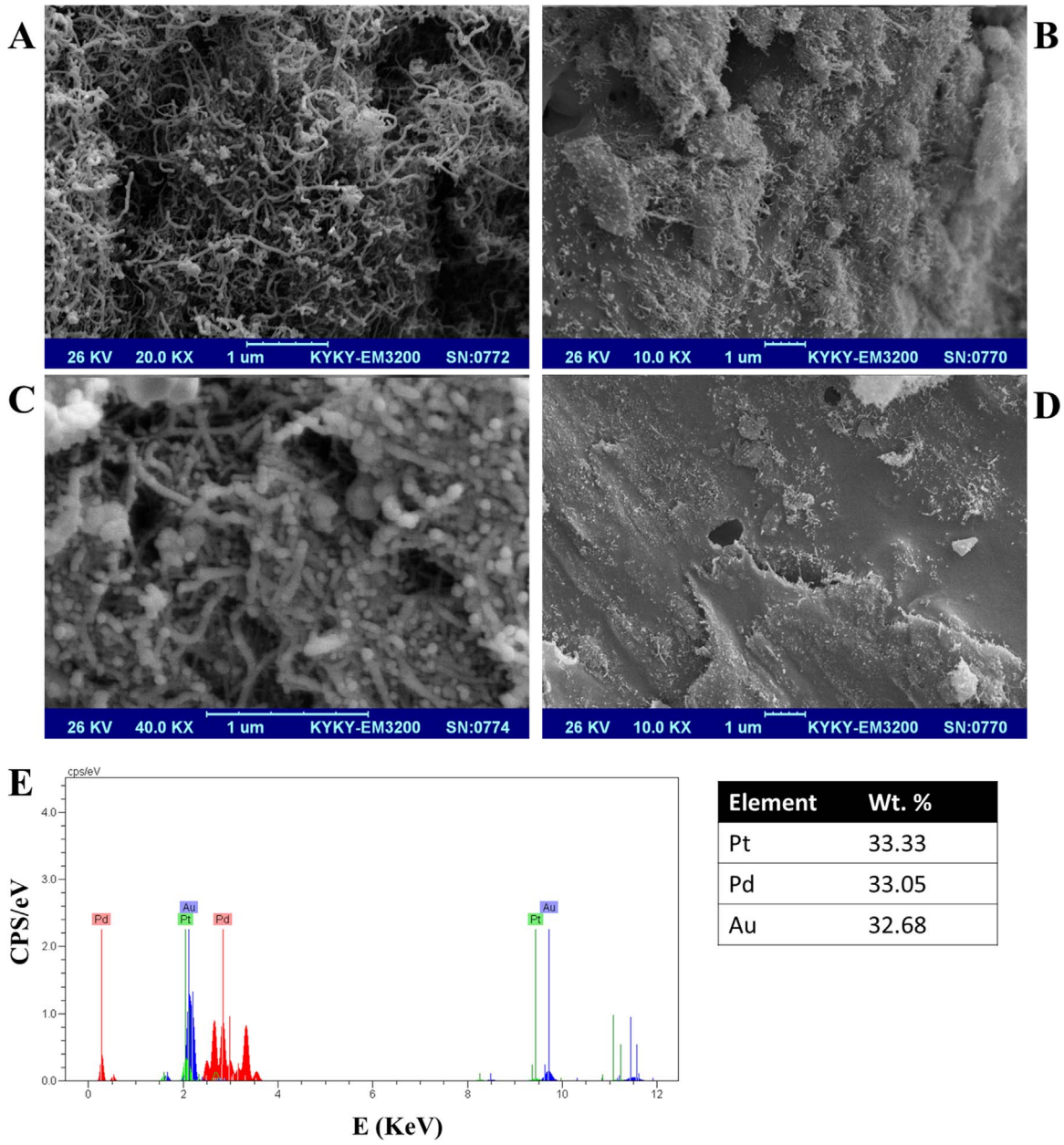

Fig. 3. The SEM image of (A) MWCNTs-IL/GCE, (B) Ch-IL/MWCNTs-IL/GCE, (C) PtAuPd NPs/Ch-IL/MWCNTs-IL/GCE and (D) HG-DDAB/PtAuPd NPs/Ch-IL/MWCNTs-IL/GCE. (D) Signature peaks obtained by EDS to characterize Pt, Au and Pd.

3.3. Investigation of the pH effects

The CVs of the biosensor (HG-DDAB/PtAuPd NPs/Ch-IL/MWCNTs-IL/GCE) immersed into the PBSs (0.05 M) with different pHs in the range from 2.0 to 12.0 were recorded in the absence of oxygen by bubbling the solution with highly pure N_2 and the results are showing in Fig. 4. As shown in Fig. 4, the CVs were negatively shifted with a slope of 58.0 mV/pH (inset of Fig. 4) by increasing the pH of the solutions in the range from 2.0 to 12.0. The slope was reasonably compatible with the theoretical value of 59.0 mV/pH for reversible one electron transfer coupled by single proton transportation [53]. As can be seen in Fig. 4, a pair of well-defined and stable redox peaks was observed for HG at pH = 7 (the CV in orange) which was selected as the optimized pH for next studies. At selected pH (pH = 7), the anodic and cathodic peaks have nearly symmetric shapes, and both of them have equal heights which suggest that all of the HG-Fe^{+3} are reduced to HG-Fe^{+2} by forward scan to negative potentials and vice versa.

3.4. Investigation of the scan rate effects

The formal potential ($E^{0'}$) of HG was estimated from its CV at pH = 7 (see Fig. 5) as the midpoint of reduction and oxidation peak potentials and was to be 0.07 V which was more positive than its formal potential at a variety of modified electrodes reported by previous studies [54–62]. The decreased formal potential of HG in our work is related to the high surface activation of the biosensor. To calculate the kinetic parameters of HG, the effects of scan rate (υ) were investigated as shown in Fig. 5A. The peak currents were regressed on scan rate values which can be observed in Fig. 5B. Regression results showed linear relationships between currents and υ (I_{pa} vs. υ, R^2 = 0.9961 and I_{pc} vs. υ, R^2 = 0.9948) which confirmed that the redox reaction was a surface-controlled process. According to the Laviron theory, the electron transfer rate constant (k_s) and the transfer coefficient (α) can be calculated from the variation of peak potential (E_p) vs. υ according to the following equation [63]:

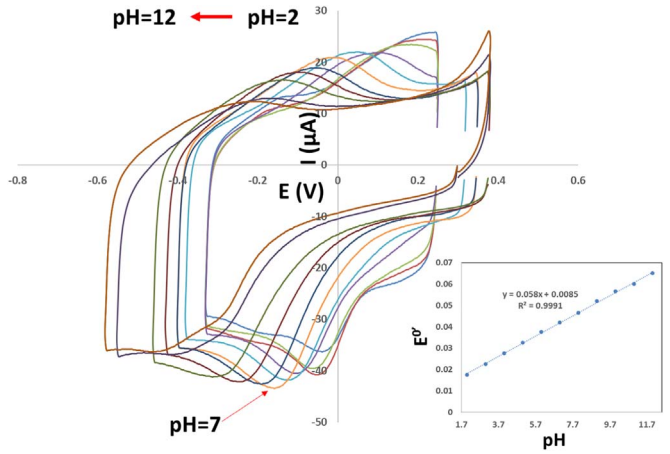

Fig. 4. CVs of HG-DDAB/PtAuPd NPs/Ch-IL/MWCNTs-IL/GCE immersed into the PBS (0.05 M) at different pHs, υ = 50.0 mVs^{-1}. Inset plot shows variation of formal potential ($E^{0'}$ = (E_{pc} + E_{pa})/2) vs. pH values.

$$E_p = E^{0'} + (RT/\alpha nF)\,[\ln(RTk_s/\alpha nF) - \ln \upsilon] \quad (1)$$

The α and k_s of HG were estimated to be 0.39 and 5.4 s^{-1} from slope and intercept of variation of ΔE_p (E_p-$E^{0'}$) vs. log (υ) (Fig. 5C), respectively. The estimated value for k_s was equal or higher than the reported values by previous studies [54–56,61,62,64,65] which showed that the electron transfer of HG at the surface of the biosensor fabricated in this study was more facile than the other electrodes.

For a reversible surface reaction, the peak current can be defined by the following equation [66]:

$$I_p = n^2F^2\nu A\Gamma_c/4RT \quad (2)$$

where v is the scan rate, A is related to the effective surface area of the electrode which is to be 0.29 cm^2 and the other symbols have their conventional meaning. The cathodic peak currents were plotted vs. scan rate and the slope of the plot was used to estimate the surface concentration (Γ_c) of HG which was to be 1.5 × 10^{-9} mol cm^{-2}.

3.5. Analytical characterizations

Since square wave voltammetry (SWV) has a much higher current sensitivity than CV especially for reversible redox reactions, it was applied to determination of AA. Under optimized conditions: step potential = −0.0025 V, amplitude = 0.05 V, frequency = 25.0 Hz, interval time = 0.04 s and scan rate = 0.0625 V/s, the relationship between SWV responses and concentrations of synthetic AA samples was investigated (Fig. 6). The difference of peak intensities ($\Delta I_p = I^*$-I, I^* = peak current in the absence of AA and I = peak current in the presence of AA) were regressed on the concentration values of AA samples (C_{AA}) and the results confirmed that there were linear relationships between I and C_{AA} over two concentration ranges from 0.03 to 39.0 nM and 39.0–150.0 nM, as can be seen in the inset of Fig. 6. The linearity observed in biosensor responses over concentration changes revealed that the biosensor could be possibly applied to the analysis of real samples for AA determination. The limit of detection (LOD) of the developed method was calculated according to IUPAC recommendations ($3S_b/b$, where S_b is the standard deviation (n = 6) of the blanks, and b refers to the slope of the calibration graph) at a concentration level of 0.01 nM. Therefore, according to the calculated LOD it can be concluded that the HG-DDAB/PtAuPd NPs/Ch-IL/MWCNTs-IL/GCE is highly sensitive. The response time of the

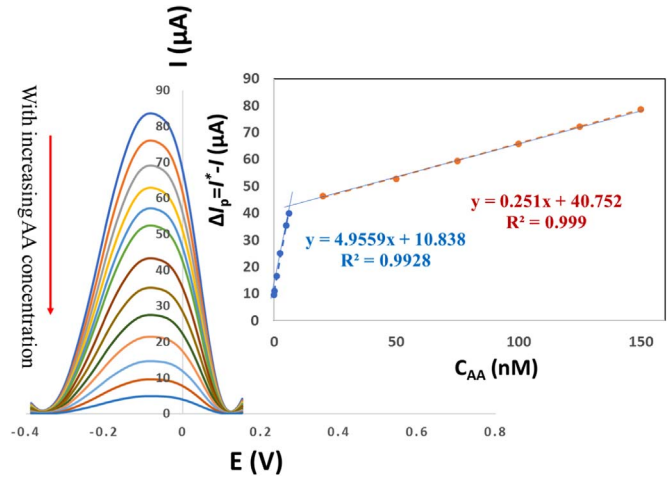

Fig. 6. SWV responses at HG-DDAB/PtAuPd NPs/Ch-IL/MWCNTs-IL/GCE upon successive additions of AA (0.03–150.0 nM) into the PBS (0.05 M, pH = 7). Inset: the linear calibration plot of difference of peak intensities ($\Delta I_p = I^*$- I, I^* = peak current in the absence of AA and I = peak current in the presence of AA) vs. concentrations of AA with two linear ranges of 0.03–39.0 nM and 39.0–50.0 nM.

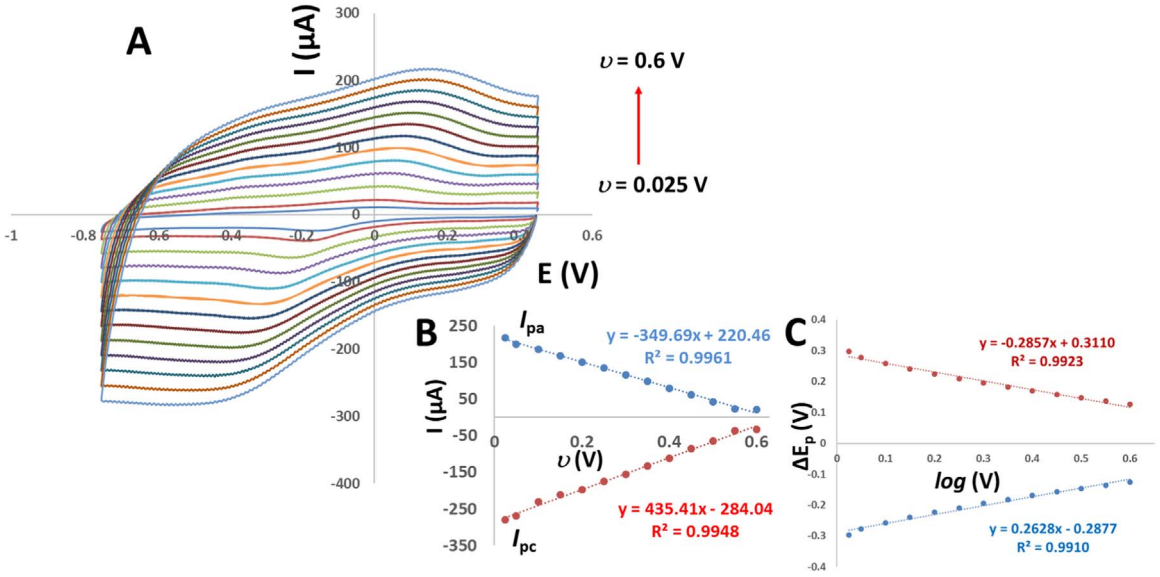

Fig. 5. (A) The CVs of HG-DDAB/PtAuPd NPs/Ch-IL/MWCNTs-IL/GCE immersed into the PBS (0.05 M, pH = 7) at different scan rates, (B) variation of peak currents vs. υ and (C) variation of ΔE_p vs. log (υ).

Table 1
Comparison of the proposed biosensor with other reported methods for AA determination.

Method	Linear range	LOD	Ref.
Hb[a]-DDAB carbon-paste modified electrode	1.3×10^{-11}–4.8×10^{-5} M	1.2×10^{-10} M	[45]
Hb-GNP[b] modified ITO glass electrode	10^{-8}–10^{-5} M	4×10^{-8} M	[67]
HPLC-MS/MS	2.8×10^{-8}–1.4×10^{-6} M	7×10^{-5} M	[68]
GC	1.4×10^{-6}–0.01 M	8×10^{-4} M	[69]
GC-MS	7×10^{-5}–7×10^{-3} M	2.8×10^{-5} M	[70]
GC-ECD	7.03×10^{-9}–1.7×10^{-6} M	1.4×10^{-6} M	[71]
GC–PCIMS/MS	1.4×10^{-8}–1.4×10^{-5} M	1.4 nM	[72]
GC-MS	7×10^{-4}–0.01 M	1.8×10^{-4} M	[73]
HPLC	7×10^{-9}–7×10^{-6} M	1 nM	[74]
FAAS	2.8×10^{-9}–2.9×10^{-6} M	7×10^{-10} M	[75]
HG-DDAB/PtAuPd NPs/Ch-IL/MWCNTs IL/GCE	0.03–39.0 nM and 39.0–150.0 nM	0.01 nM	This work

[a] Hemoglobin.
[b] Gold nano particles.

biosensor was also investigated and the results showed that it was less than 8 s.

3.6. Comparison with previous works reported in literature

The results obtained by the proposed biosensor in this study were compared with those of previous works reported in the literature and are presented in Table 1. As can be seen, the proposed biosensor showed better results over the most of the reported methods even in comparison to chromatographic techniques.

3.7. Interference study

Studying the interfering effects of several compounds including 2-nitrobenzaldehyde, acetaldehyde, hydrazine, phenol, acetate, ascorbic acid, tartrate and bromobenzaldehyde which are commonly existed in food samples are very necessary to investigate the matrix effects on AA determination by the proposed method in this study. Therefore, a tolerance limit of an interfering compound was defined as the concentration which gave an error of 5.0% in determination of AA at level of 30.0 nM. Afterwards, the effects of interfering compounds on AA determination were investigated under the optimized conditions by computing the recoveries of the AA. The results are shown in Table 2. As can be seen, the presences of large amounts of interfering compounds had no significant matrix effect on AA determination by the proposed biosensor in this study.

Table 2
Effect of potential interfering ions on the recovery of the AA at level of 30.0 nM.

Interfering spices	Concentration of added interfering spices	Recovery of AA (%)
2-nitrobenzaldehyde	10 μM	98
Acetaldehyde	35 μM	101
Hydrazine	5 μM	104
Phenol	20 μM	102
Acetate	20 μM	97
Ascorbic acid	40 μM	100
Tartrate	10 μM	98
Bromobenzaldehyde	5 μM	102

3.8. Stability, repeatability and reproducibility of the biosensor

Stability is one the most important characteristics of a biosensor therefore, to investigate the stability of HG-DDAB/PtAuPd NPs/Ch-IL/MWCNTs-IL/GCE, a solution containing 30.0 nM AA was prepared in the PBS (0.05 M, pH 7.0) and analyzed by SWV. After two weeks, the proposed biosensor retained 95.3% of its initial response. After four weeks, the biosensor retained 93.7% of its original response. It was also observed that the stability of the biosensor could be affected by the time of immersing into the solution therefore, this parameter was also investigated and the results confirmed that the stability of the biosensor is highly affected by a long time of immersing into the solution and the biosensor doesn't show a good stability by immersing into the cell solution for more than 5.0 h. Therefore, our recommendation to tackle this challenge is to remove the biosensor from cell solution during the breaks between the experiments. To investigate the repeatability of the proposed biosensor, it was applied for ten times during a day to determine AA in the same solution used for stability verification and a satisfied relative standard deviation (RSD) of 2.9% which confirmed a good repeatability was obtained. The reproducibility of the biosensor was also investigated by recording the SWV responses of eight individual biosensors immersed into a solution containing 30.0 nM AA prepared in the PBS (0.05 M, pH 7.0) and an acceptable RSD value of 3.8% was obtained which guaranteed a good reproducibility for the biosensor. The results mentioned above, confirmed that the biosensor response towards AA determination is stable, repeatable, and reproducible.

3.9. Analysis of real samples

To evaluate the performance of the developed biosensor for the analysis of real samples, the biosensor was used to determine AA in potato crisp samples using SWV technique. 5.2 mL of the solution prepared according to the procedure described in Section 2.4 was diluted to 10.4 mL by the addition of PBS (0.05 M, pH 7.0) and transferred into an electrochemical cell with Ag/AgCl, Pt wire and HG-DDAB/PtAuPd NPs/Ch-IL/MWCNTs-IL/GCE as its reference, counter and working electrodes, respectively. Furthermore, spiked real samples were also analyzed to prove the practical application of the fabricated biosensor towards AA determination. Results of the analysis of real samples are presented in Table 3. Analysis of spiked samples showed excellent recoveries which confirmed the appreciable practical feasibility of the biosensor towards AA determination in real matrices.

When a new analytical method is developed, its performance must be compared with a reference method and with regarding this important step, we also applied GC-MS for the analysis of the real samples and its results are presented in Table 3. To make a graphically comparison between accuracy and precision of the GC-MS and the proposed biosensor, we used the EJCR test [76,77]. To achieve this goal, the predicted concentrations by the proposed biosensor and/or GC-MS were regressed on the nominal concentrations (added concentrations) by ordinary least squares (OLS). Then, the EJCR test was used to compare the calculated intercept and slope with their expected values (intercept = 0, slope = 1) which is also called "the ideal point". Therefore, if the ellipses obtained by the EJCR include the ideal point, the predicted and nominal values are not significantly different. The size of ellipses refers to the precision of the method, smaller sizes confirm higher precisions [76,77]. Results of the EJCR test are showing in Fig. 7. As can be seen, ellipses of both methods contain the ideal point which confirm that both of them are accurate but, the ellipse of GC-MS is smaller than that of the proposed biosensor which confirms that the GC-MS precision is slightly better than the proposed biosensor as confirmed by the results reported in Table 3.

According to the results obtained above, the GC-MS was slightly better than the proposed biosensor but, by regarding the disadvantages of the GC-MS such as cost, time and requiring a highly skilled operator,

Table 3
Determination of AA in real samples using the proposed biosensor and GC-MS as reference method.

Sample	Analytical method	Detected	Added (nM)	Found (nM)	Recovery (%)
Maz Maz	Proposed Biosensor	N.D[a]	50, 120, 15, 140	50.7, 119.2, 15.06, 139.1	101.4, 99.9, 100.4, 99.36
	GC-MS	N.D	50, 120, 15, 140	50.1, 120.2, 15.02, 140.1	100.2, 100.2, 100.1, 100.07
	Proposed Biosensor	N.D	25, 85, 100, 10	25.03, 85.7, 99.6, 9.88	100.1, 100.8, 99.6, 98.8
Chee Toz	GC-MS	N.D	25, 85, 100, 10	25, 85.1, 100.4, 9.92	100.0, 100.1, 100.4, 99.2

[a] Not detected.

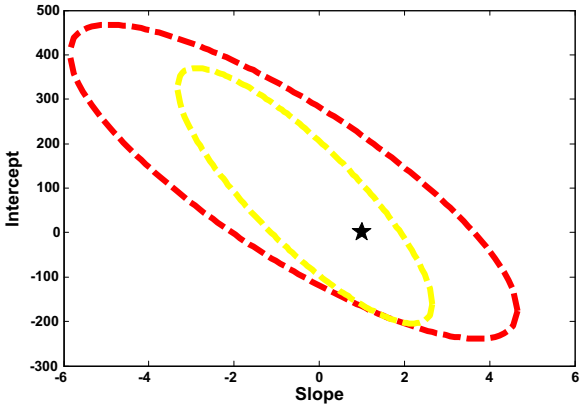

Fig. 7. Elliptical joint confidence regions (at 95% confidence level) for the slopes and intercepts of the regressions for AA determination in spiked real samples. Red ellipse: proposed biosensor, yellow ellipse: GC-MS and star point marks the ideal point (0,1). (For interpretation of the references to color in this figure legend, the reader is referred to the web version of this article.)

the proposed biosensor is suggested for the analysis of real samples towards AA determination.

4. Conclusions

A novel electrochemical biosensor based on formation of a HG-AA adduct for determination of AA in food samples was fabricated. The decrease of the peak intensity of reduction of HG-Fe^{3+} to HG-Fe^{2+} caused by increasing concentration of AA was used as the analytical signal. Platform of the biosensor is a GCE with interesting modifications (HG-DDAB/PtAuPd NPs/Ch-IL/MWCNTs-IL/GCE) to provide high selectivity and sensitivity, short response time, long term stability, good repeatability and reproducibility towards AA determination. Formation of the HG-AA adduct caused a high selectivity for the biosensor and the matrix of real samples had no influence on the electrochemical response of the biosensor. The presence of PtAuPd alloy NPs in addition to increasing the sensitivity can help to the stability of the biosensor by the adsorption of HG onto the biosensor surface via the interaction between cysteine or $NH^{+}{}_{4}$-lysine residues of HG and Au NPs. Ch-IL enhances the nucleation rate which facilitates formation of smaller NPs, and MWCNTs-IL is able to increase the sensitivity of the biosensor. On the whole, intellectual designing the biosensor structure helped us to develop a novel analytical method for sensitive and selective determination of AA in food samples which its results were comparable to those obtained by the GC-MS as reference method. The methodology developed in this study might be applied for a wide range of real samples in relation to the detection of AA.

Compliance with ethics requirements

This work does not have any studies with humans or animals.

Conflict of interests

Here, we declare that we have no conflict of interest.

Acknowledgements

Financial supports of this project by the Research Council of Kermanshah University Of Medical Sciences are gratefully acknowledged.

References

[1] N. Altunay, R. Gürkan, U. Orhan, A preconcentration method for indirect determination of acrylamide from chips, crackers and cereal-based baby foods using flame atomic absorption spectrometry, Talanta 161 (2016) 143–150.
[2] A. Claus, C. Reinhold, S. Andreas, Acrylamide in cereal products: a review, J. Cereal Sci. 47 (2008) 118–133.
[3] D.S. Mottram, B.L. Wedzicha, A.T. Dodson, Food chemistry: acrylamide is formed in the Maillard reaction, Nature 419 (2002) 448–449.
[4] E. Tareke, P. Rydberg, P. Karlsson, S. Eriksson, M. Törnqvist, Analysis of acrylamide, a carcinogen formed in heated foodstuffs, J. Agric. Food Chem. 50 (2002) 4998–5006.
[5] W.L. Claeys, K. De Vleeschouwer, M.E. Hendrickx, Kinetics of acrylamide formation and elimination during heating of an asparagine-sugar model system, J. Agric. Food Chem. 53 (2005) 9999–10005.
[6] IARC monographs on the evaluation of carcinogenic risks to humans 60, Some Industrials Chemicals, International Agency for Research on Cancer, Lyon, France, 1994, pp. 389–433.
[7] Report of a Joint FAO/WHO Consultation WHO Headquarters, Geneva, Switzerland, 2002.
[8] A.R. Ghiasvand, S. Hajipour, Direct determination of acrylamide in potato chips by using headspace solid-phase microextraction coupled with gas chromatography-flame ionization detection, Talanta 146 (2016) 417–422.
[9] S. Lee, M. Yoo, M. Koo, H.J. Kim, M. Kim, S.K. Park, D. Shin, In-house-validated liquid chromatography-tandem mass spectrometry (LC-MS/MS) method for survey of acrylamide in various processed foods from Korean market, Food Sci. Nutr. 1 (2013) 402–407.
[10] R. Bortolomeazzi, M. Munari, M. Anese, G. Verardo, Rapid mixed mode solid phase extraction method for the determination of acrylamide in roasted coffee by HPLC-MS/MS, Food Chem. 135 (2012) 2687–2693.
[11] Y. Zhang, Y. Ren, J. Jiao, D. Li, Y. Zhang, Ultra high-performance liquid chromatography-tandem mass spectrometry for the simultaneous analysis of asparagine, sugars, and acrylamide in Maillard reactions, Anal. Chem. 83 (2011) 3297–3304.
[12] M.V. Russo, P. Avino, A. Centola, I. Notardonato, G. Cinelli, Rapid and simple determination of acrylamide in conventional cereal-based foods and potato chips through conversion to 3-[bis (trifluoroethanoyl) amino]-3-oxopropyl trifluoroacetate by gaschromatography coupled with electron capture and ion trap mass spectrometry detectors, Food Chem. 146 (2014) 204–211.
[13] M.R. Lee, L.Y. Chang, J. Dou, Determination of acrylamide in food by solid-phase microextraction coupled to gas chromatography–positive chemical ionization tandem mass spectrometry, Anal. Chim. Acta 582 (1) (2007) 19–23.
[14] Y. Yamini, M. Ghambarian, A. Esrafili, N. Yazdanfar, M. Moradi, Rapid determination of ultra-trace amounts of acrylamide contaminant in water samples using dispersive liquid-liquid microextraction coupled to gas chromatography-electron capture detector, Int. J. Environ. Anal. Chem. 92 (2012) 1493–1505.
[15] M. Kaykhaii, A. Abdi, Rapid and sensitive determination of acrylamide in potato crisps using reversed-phase direct immersion single drop microextraction-gas chromatography, Anal. Methods 5 (2013) 1289–1293.
[16] F. Zhu, Y.Z. Cai, J. Ke, H. Corke, Evaluation of the effect of plant extracts and phenolic compounds on reduction of acrylamide in an asparagine/glucose model system by RP-HPLCDAD, J. Sci. Food Agric. 89 (2009) 1674–1681.
[17] I.G. Casella, M. Pierri, M. Contursi, Determination of acrylamide and acrylic acid by isocratic liquid chromatography with pulsed electrochemical detection, J. Chromatogr. A 1107 (2006) 198–203.
[18] M.J.A. Shiddiky, A.A.J. Torriero, Application of ionic liquids in electrochemical sensing systems, Biosens. Bioelectron. 26 (2011) 1775–1787.
[19] H.Y. Gu, A.M. Yu, H.Y. Chen, Direct electron transfer and characterization of hemoglobin immobilized on a Au colloid-cysteamine-modified gold electrode, J. Electroanal. Chem. 516 (2001) 119–126.
[20] J.M. Pingarron, P. Yanez-Sedeno, A. Gonzales-Cortez, Gold nanoparticle-based electrochemical biosensors, Electrochim. Acta 53 (2008) 5848–5866.
[21] A. Stobiecka, H. Radecka, J. Radecki, Novel voltammetric biosensor for determining acrylamide in food samples, Biosens. Bioelectron. 22 (2007) 2165–2170.

[22] C. Zhao, L. Wan, L. Jiang, Q. Wang, K. Jiao, Highly sensitive and selective cholesterol biosensor based on direct electron transfer of hemoglobin, Anal. Biochem. 383 (2008) 25–30.
[23] X. Ma, X. Liu, H. Xiao, G. Li, Direct electrochemistry and electrocatalysis of hemoglobin in poly-3-hydroxybutyrate membrane, Biosens. Bioelectron. 20 (2005) 1836–1842.
[24] A. Krajewska, J. Radecki, H. Radecka, A voltammetric biosensor based on glassy carbon electrodes modified with single-walled carbon nanotubes/hemoglobin for detection of acrylamide in water extracts from potato crisps, Sensors 8 (2008) 5832–5844.
[25] W. Cheng, G. Jin, Y. Zhang, Direct electron transfer of hemoglobin on PSS/SWNTs film modified Au electrode and its interaction with ribavirin, Sens. Actuators B 114 (2006) 40–46.
[26] J. Zhang, M. Oyama, A hydrogen peroxide sensor based on the peroxidase activity of hemoglobin immobilized on gold nanoparticles-modified ITO electrode, Electrochim. Acta 50 (2004) 85–90.
[27] J. Zhang, M. Oyama, A novel electrode surface fabricated by directly attaching gold nanospheres and nanorods onto indium tin oxide substrate with a seed mediated growth process, Electrochem. Commun. 6 (2004) 683–688.
[28] Y. Wang, W. Qian, Y. Tang, S. Ding, H. Zhang, Direct electrochemistry and electroanalysis of hemoglobin adsorbed in self-assembled films of gold nanoshells, Talanta 72 (2007) 1134–1140.
[29] L. Zhang, X. Jiang, E. Wang, S. Dong, Attachment of gold nanoparticles to glassy carbon electrode and its application for the direct electrochemistry and electrocatalytic behavior of hemoglobin, Biosens. Bioelectron. 21 (2005) 337–345.
[30] G. Yang, R. Yuan, Y.Q. Chai, A high-sensitive amperometric hydrogen peroxide biosensor based on the immobilization of hemoglobin on gold colloid/L-cysteine/gold colloid/nanoparticles Pt–chitosan composite film-modified platinum disk electrode, Colloids Surf. B: Biointerfaces 61 (2008) 93–100.
[31] Y. Xu, C. Hu, S. Hu, A reagentless nitric oxide biosensor based on the direct electrochemistry of hemoglobin adsorbed on the gold colloids modified carbon paste electrode, Sens. Actuators B 148 (2010) 253–258.
[32] W. Wang, T.J. Zhang, D.W. Zhang, H.Y. Li, Y.R. Ma, L.M. Qi, Y.L. Zhou, X.X. Zhang, Amperometric hydrogen peroxide biosensor based on the immobilization of heme proteins on gold nanoparticles–bacteria cellulose nanofibers nanocomposite, Talanta 84 (2011) 71–77.
[33] S. Liu, Z. Dai, H. Chen, H. Ju, Immobilization of hemoglobin on zirconium dioxide nanoparticles for preparation of a novel hydrogen peroxide biosensor, Biosens. Bioelectron. 19 (2004) 963–969.
[34] H.H. Liu, Z.Q. Tian, Z.X. Lu, Z.L. Zhang, M. Zhang, D.W. Pang, Biosens. Bioelectron. 20 (2004) 294–304.
[35] G.A. Rivas, M.D. Rubianes, M.C. Rodrıguez, N.F. Ferreyra, G.L. Luque, M.L. Pedano, S.A. Miscoria, C. Parrado, Carbon nanotubes for electrochemical biosensing, Talanta 74 (2007) 291–307.
[36] M.C. Buzzeo, R.G. Evans, R.G. Compton, Non-haloaluminate room-temperature ionic liquids in electrochemistry–a review, Chem. Phys. Chem. 5 (2004) 1106–1120.
[37] N. Maleki, A. Safavi, F. Tajabadi, High-performance carbon composite electrode based on an ionic liquid as a binder, Anal. Chem. 78 (2006) 3820–3826.
[38] Z. Zhu, L. Qu, X. Li, Y. Zeng, W. Sun, X. Huang, Direct electrochemistry and electrocatalysis of hemoglobin with carbon nanotube-ionic liquid-chitosan composite materials modified carbon ionic liquid electrode, Electrochim. Acta 55 (2010) 5959–5965.
[39] A. Safavi, F. Farjami, Electrodeposition of gold-platinum alloy nanoparticles on ionic liquid-chitosan composite film and its application in fabricating an amperometric cholesterol biosensor, Biosens. Bioelectron. 26 (2011) 2547–2552.
[40] R.K. Katarina, T. Takayanagi, M. Oshima, S. Motomizu, Synthesis of a chitosan-based chelating resin and its application to the selective concentration and ultratrace determination of silver in environmental water samples, Anal. Chim. Acta 558 (2006) 246–253.
[41] O.B. Mokhodoeva, G.V. Myasoedova, I.V. Kubrakova, Sorption preconcentration in combined methods for the determination of noble metals, J. Anal. Chem. 62 (2007) 607–622.
[42] X. Kang, Z. Mai, X. Zou, P. Cai, J. Mo, A novel glucose biosensor based on immobilization of glucose oxidase in chitosan on a glassy carbon electrode modified with gold-platinum alloy nanoparticles/multiwall carbon nanotubes, Anal. Biochem. 369 (2007) 71–79.
[43] F. Xiao, F. Zhao, Y. Zhang, G. Guo, B. Zeng, Ultrasonic electrodeposition of gold–platinum alloy nanoparticles on ionic liquid–chitosan composite film and their application in fabricating nonenzyme hydrogen peroxide sensors, J. Phys. Chem. C 113 (2009) 849–855.
[44] J. Yang, S. Deng, J. Lei, H. Jub, S. Gunasekaran, Electrochemical synthesis of reduced graphene sheet-AuPd alloy nanoparticle composites for enzymatic biosensing, Biosens. Bioelectron. 29 (2011) 159–166.
[45] A. Stobiecka, H. Radecka, J. Radecki, Novel voltammetric biosensor for determining acrylamide in food samples, Biosens. Bioelectron. 22 (2007) 2165–2170.
[46] A. Krajewska, J. Radecki, H. Radecka, A voltammetric biosensor based on glassy carbon electrodes modified with single-walled carbon nanotubes/hemoglobin for detection of acrylamide in water extracts from potato crisps, Sensors 8 (2008) 5832–5844.
[47] H.Y. Gu, A.M. Yu, H.Y. Chen, Direct electron transfer and characterization of hemoglobin immobilized on a Au colloid–cysteamine-modified gold electrode, J. Electroanal. Chem. 516 (2001) 119–126.
[48] J.F. Rusling, Enzyme bioelectrochemistry in cast biomembrane-like films Acc. Chem., Res. 31 (1998) 363–369.
[49] M. Bayachou, R. Lin, W. Cho, P.J. Farmer, Electrochemical reduction of NO by myoglobin in surfactant film: characterization and reactivity of the nitroxyl (NO-) adduct, J. Am. Chem. Soc. 120 (1998) 9888–9893.
[50] D. Mimica, J.H. Zagal, F. Bedioui, Electroreduction of nitrite by hemin, myoglobin and hemoglobin in surfactant films, J. Electroanal. Chem. 497 (2001) 106–113.
[51] D. Mimica, J.H. Zagal, F. Bedioui, Electrocatalysis of nitric oxide reduction by hemoglobin entrapped in surfactant films, Electrochem. Commun. 3 (2001) 435–438.
[52] S.M. Chen, C.C. Tseng, The characterization and bioelectrocatalytic properties of hemoglobin by direct electrochemistry of DDAB film modified electrodes, Electrochim. Acta 49 (2004) 1903–1907.
[53] L. Meites, Polarographic Techniques, Wiley, New York, 1965.
[54] H. Lu, Z. Li, N. Hu, Direct voltammetry and electrocatalytic properties of catalase incorporated in polyacrylamide hydrogel films, Biophys. Chem. 104 (2003) 623–632.
[55] X. Ma, X. Liu, H. Xiao, G. Li, Hydrogen peroxide biosensor based on the direct electrochemistry of myoglobin immobilized in poly-3-hydroxybutyrate film, Biosens. Bioelectron. 20 (2005) 1836–1842.
[56] L. Shen, N. Hu, Heme protein films with polyamidoamine dendrimer: direct electrochemistry and electrocatalysis, Biochim. Biophys. Acta 2004 (1608) 23–33.
[57] X. Liu, Y. Xu, X. Ma, G. Li, A third-generation hydrogen peroxide biosensor fabricated with hemoglobin and triton X-100, Sens. Actuators B 106 (2005) 284–288.
[58] X. He, L. Zhu, Direct electrochemistry of hemoglobin in cetylpyridinium bromide film: redox thermodynamics and electrocatalysis to nitric oxide, Electrochem. Commun. 8 (2006) 615–620.
[59] S.M. Chen, C.C. Tseng, Comparison of the direct electrochemistry of myoglobin and hemoglobin films and their bioelectrocatalytic properties, J. Electroanal. Chem. 575 (2005) 147–160.
[60] C. Fan, H. Wang, S. Sun, D. Zhu, G. Wagner, G. Li, Electron-transfer reactivity and enzymatic activity of hemoglobin in a SP sephadex membrane, Anal. Chem. 73 (2001) 2850–2854.
[61] H.Y. Gu, A.M. Yu, H.Y. Chen, Direct electron transfer and characterization of hemoglobin immobilized on a Au colloid–cysteamine-modified gold electrode, J. Electroanal. Chem. 516 (2001) 119–126.
[62] J.J. Feng, J.J. Xu, H.Y. Chen, Direct electron transfer and electrocatalysis of hemoglobin adsorbed onto electrodeposited mesoporous tungsten oxide, Electrochem. Commun. 8 (2005) 77–82.
[63] E. Laviron, General expression of the linear potential sweep voltammogram in the case of diffusionless electrochemical systems, J. Electroanal. Chem. 101 (1979) 19–28.
[64] Y. Zhou, Z. Li, N. Hu, Y. Zeng, J.F. Rusling, Layer-by-layer assembly of ultrathin films of hemoglobin and clay nanoparticles with electrochemical and catalytic activity, Langmuir 18 (2002) 8573–8579.
[65] Q. Li, G. Luo, J. Feng, Direct electron transfer for heme proteins assembled on nanocrystalline TiO_2 film, Electroanalysis 13 (2001) 359–363.
[66] J. Wang, Analytical Electrochemistry, VCH, New York, 1999.
[67] S. Garabagiu, G. Mihailescu, Simple hemoglobin-gold nanoparticles modified electrode for the amperometric detection of acrylamide, J. Electroanal. Chem. 659 (2011) 196–200.
[68] R. Bortolomeazzi, M. Munari, M. Anese, G. Verardo, Rapid mixed mode solid phase extraction method for the determination of acrylamide in roasted coffee by HPLC-MS/MS, Food Chem. 135 (2012) 2687–2693.
[69] M. Kaykhaii, A. Abdi, Rapid and sensitive determination of acrylamide in potato crisps using reversed-phase direct immersion single drop microextraction-gas chromatography, Anal. Methods 5 (2013) 1289–1293.
[70] A. Pittet, A. Périsset, J.M. Oberson, Trace level determination of acrylamide in cereal based foods by gas chromatography–mass spectrometry, J. Chromatogr. A 1035 (2004) 123–130.
[71] Y. Zhang, Y. Dong, Y. Ren, Y. Zhang, Rapid determination of acrylamide contaminant in conventional fried foods by gas chromatography with electron capture detector, J. Chromatogr. A 1116 (2006) 209–216.
[72] M.R. Lee, L.Y. Chang, J. Dou, Determination of acrylamide in food by solid-phase microextraction coupled to gas chromatography–positive chemical ionization tandem mass spectrometry, Anal. Chim. Acta 582 (2007) 19–23.
[73] M.M.A. Omar, W.A.W. Ibrahim, A.A. Elbashir, Sol-gel hybrid methyltrimethoxysilane-tetraethoxysilane as a new dispersive solid-phase extraction material for acrylamide determination in food with direct gas chromatography-mass spectrometry analysis, Food Chem. 158 (2014) 302–309.
[74] L. Xu, X. Qiao, Y. Ma, X. Zhang, Z. Xu, Preparation of a hydrophilic molecularly imprinted polymer and its application in solid-phase extraction to determine of trace acrylamide in foods coupled with high-performance liquid chromatography, Food Anal. Methods 6 (2013) 838–844.
[75] N. Altunay, R. Gürkan, U. Orhan, A preconcentration method for indirect determination of acrylamide from chips, crackers and cereal-based baby foods using flame atomic absorption spectrometry, Talanta 161 (2016) 143–150.
[76] A.G. Gonzalez, M.A. Herrador, A.G. Asuero, Intra-laboratory testing of method accuracy from recovery assays, Talanta 48 (1999) 729–736.
[77] J.A. Arancibia, G.M. Escandar, Two different strategies for the fluorimetric determination of piroxicam in serum, Talanta 60 (2003) 1113–1121.